


Dual-band B-shaped antenna array for satellite applications

cambridge.org/mrf

Muhammad Mateen Hassan , Muzhair Hussain, Adnan Ahmed Khan,
Imran Rashid and Farooq Ahmed Bhatti

Department of Electrical Engineering, Military College of Signals, National University of Sciences and Technology, Rawalpindi, Pakistan

Research Paper

Cite this article: Hassan MM, Hussain M, Khan AA, Rashid I, Bhatti FA (2021). Dual-band B-shaped antenna array for satellite applications. *International Journal of Microwave and Wireless Technologies* **13**, 851–858. <https://doi.org/10.1017/S1759078720001439>

Received: 18 April 2020
Revised: 21 September 2020
Accepted: 22 September 2020
First published online: 19 October 2020

Key words:

Dual-band; antenna array; satellite communication

Author for correspondence:

Muhammad Mateen Hassan, E-mail: mmateenhassan@gmail.com

Abstract

The paper presents a 1×2 B-shaped antenna array for dual-band operation at 4 and 8 GHz. The antenna design consists of a rectangular patch with two annular-strip lines fabricated on the top layer and finite ground plane on the bottom layer. The array is formed by designing an optimum T-shaped microstrip line for impedance matching. The dimensions of the antenna array are $78 \times 36 \times 1.6 \text{ mm}^3$. Full-wave simulations have been conducted and the measured results are in good consent with the simulated results. The measured impedance bandwidth (reference -10 dB) has been observed at 3.84–4.16 and 7.78–8.38 GHz. Measured peak gain and radiation efficiency at 4 and 8 GHz are 8.3, 9.4 dB and 82.5 and 81.2%, respectively.

Introduction

Satellite communication plays a vital role in delivering wireless communication services to live TV broadcasting, weather radar system, and internet services [1]. International Telecommunication Union (ITU) has divided the world into three regions for satellite communication. In region 3, ITU has allocated 3.7–4.2 and 7.9–8.4 GHz for downlink communication and uplink communication in fixed satellite service. Instead of using multiple antennas, satellite communication requires a single antenna with dual-band operation [2, 3]. To overcome the issue, researches proposed microstrip antennas for dual-band performance [4, 5].

Several dual-band antennas (non-array) had been reported in the literature. For instance, in [6] a microstrip antenna was proposed for dual-band operation at 0.6–0.8 and 1.1–1.9 GHz. The dual-band behavior was achieved by adding a shorting pin and slots in the radiating patch. Rectangular patch antenna loaded with D-shaped complementary split-ring resonators etched in the ground plane for dual-band operation was presented in [7]. An F-shaped patch antenna with defected ground structure (DGS) and double squared strip for tri-band operation at 4.6, 7.3, and 11.1 GHz was discussed in [8]. In [9], a circular patch on a half hemispherical dielectric resonator antenna was proposed for 4.5 and 5.3 GHz, respectively. A planar inverted F antenna for dual-band performance was proposed in [10]. Dual-band operation was achieved by inserting S-shaped and T-shaped slots in the radiating patch and the ground plane. A slot antenna with C-shaped strip in the ground plane was proposed for dual-band operation at 1.4 and 2.4 GHz [11]. A circular patch antenna surrounded by mushroom-shaped strips was presented in [12]. Vallappil *et al.* [13] proposed a Minkowski–Sierpinski-shaped antenna for dual-band operation. Peak gain at 4 and 5.9 GHz was 0.4 and 6.2 dB, respectively. A square quadrifilar helix antenna was presented in [14] for dual-band behavior at 1.2 and 1.5 GHz. Spiral antenna with the frequency-selective surface (FSS) was proposed for dual-band performance at 1.8 and 3.5 GHz [15]. Asif *et al.* [16] proposed an E-shaped microstrip patch antenna for dual-band characteristics. A triangular slot antenna using substrate-integrated waveguide (SIW) for dual-band operation at 9.5 and 12 GHz was discussed in [17]. Inverted U-shaped slot antenna using SIW was proposed for dual-band performance [18]. Peak gain at 4.2 and 7.5 GHz was 5.3 and 5.8 dB, respectively. A monopole antenna with two sleeves was introduced in [19] for dual-band operation. Rectangular patch antenna using multiple substrates for dual-band operation was highlighted in [20]. Dual-band performance was achieved by inserting multiple slots in the radiating patch which were discussed in [21, 22]. A planar antenna for dual-band operation using DGS and meander lines structure was proposed in [23].

Several dual-band antenna arrays had existed in the literature. A helical antenna array for dual-band operation at 1.65 and 1.75 GHz was discussed in [24]. A continuous transverse stub antenna array was proposed in [25] for tri-band operation. Peak gain at 5.1, 6.5, and 7.4 GHz was 7.5, 5.2, and 7.5 dB, respectively. A 4×4 electrically steerable passive array radiator was proposed for dual-band operation at wireless local area network (WLAN) and worldwide interoperability for microwave access (WiMAX) bands [26]. A 4×4 tightly coupled dipole antenna array was presented in [27]. A shared aperture stacked antenna array was proposed

© The Author(s), 2020. Published by Cambridge University Press in association with the European Microwave Association

CAMBRIDGE
UNIVERSITY PRESS

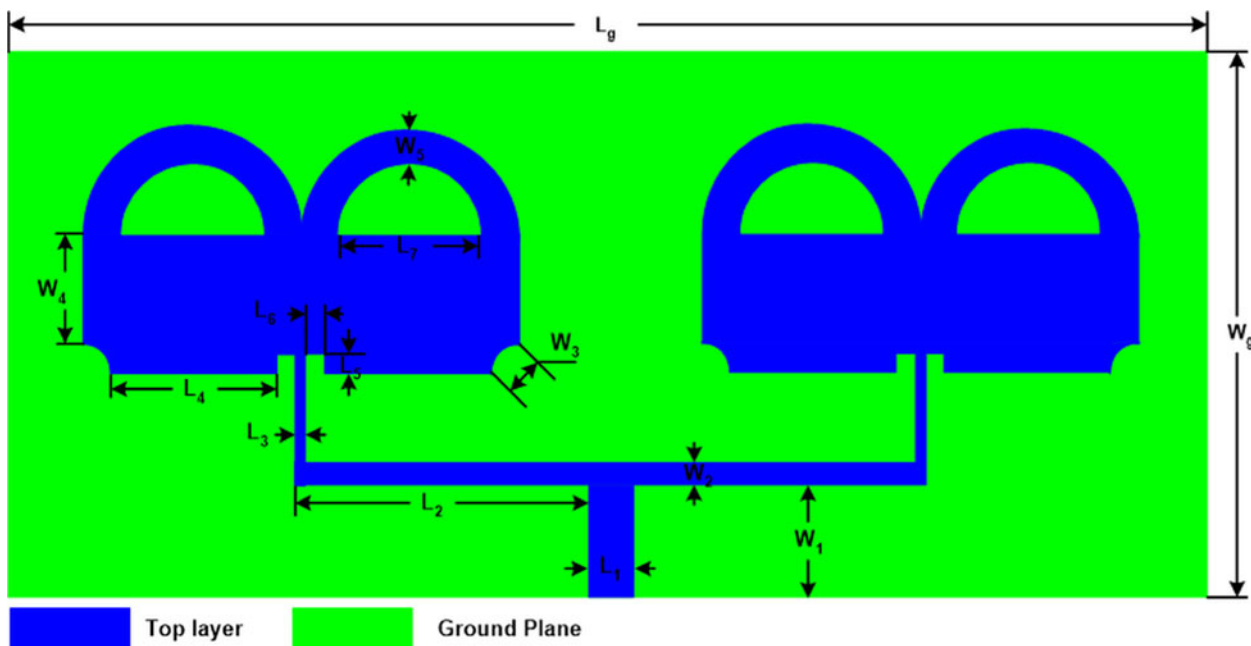


Fig. 1. Geometry of the proposed B-shaped antenna array.

Table 1. Dimensions of the proposed B-shaped antenna array

Parameter	L_g	W_g	L_1	L_2	L_3	L_4	L_5	L_6	L_7	W_1	W_2	W_3	W_4	W_5
Value (mm)	78	35	2.9	19.2	1	10.7	1.2	1.3	9.2	7.1	1.5	2.5	7.1	2.5

for dual-band operation in [28]. In [29], aperture shared microstrip antenna array for a dual-band operation was discussed. A 3×2 folded dipole antenna array was proposed in [30] for dual-band operation in WLAN and WiMAX bands. A 7×7 spanner-shaped FSS was designed and placed over a slot antenna for dual-band behavior at 3.5 and 6.2 GHz [31]. A dome-shaped antenna array was discussed in [32] for dual-band operation at 5.8 and 7.8 GHz. A 4×4 H-shaped co-aperture antenna array was presented in [33] for dual-band performance.

The existed literature focused on multi-substrate layers and complex structure design for dual-band operation. Therefore, a wide bandwidth with high gain is an active area of research. In this endeavor, a wide band and high gain dual-band B-shaped antenna array is proposed. The simulated impedance bandwidth (reference -10 dB) is observed at 3.7–4.2 and 7.7–8.4 GHz, respectively. The proposed B-shaped antenna array is fabricated on low-cost FR4 substrate and good consent between measured results and simulated results is observed.

Antenna array design

The proposed geometry of 1×2 B-shaped antenna array is shown in Fig. 1. The design consists of a modified rectangular patch antenna on one side of the substrate and finite ground plane on the other side. The antenna is fabricated on FR4 substrate ($\epsilon_r = 4.4$, loss tangent 0.02, thickness $0.02\lambda_o$, where λ_o denotes the free space wavelength at 4 GHz). The antenna array is fed by the microstrip line with 50Ω characteristics impedance. The microstrip line terminates at T-shaped impedance-matching microstrip line [34] whose values have been optimized in the

simulator. The inset feed line and the round edges have been used for wide band impedance matching. Two annular-shaped strip lines have been attached on the rectangular patch to obtain dual-band and wide band characteristics. Simulations have been carried out in CST Microwave Studio 16 [35]. The dimensions of the proposed antenna array are illustrated in Table 1.

Parametric study

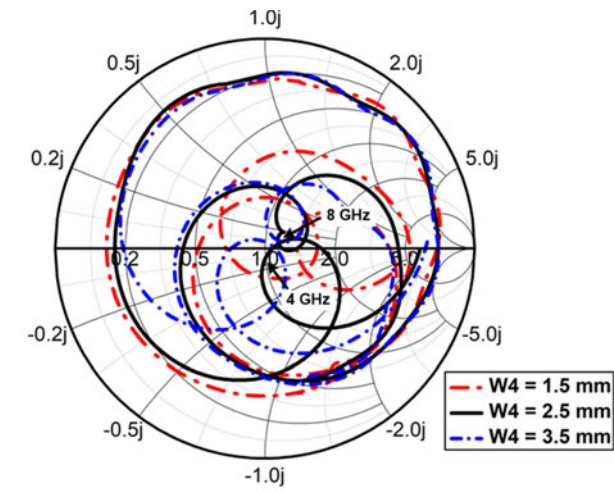
The impact of the B-shaped patch antenna has been further analyzed in this section. The length of parameter W_4 has been varied and the reflection coefficient is shown in Fig. 2. Reflection coefficient plotted on Smith chart for $W_4 = 1.5, 2.5$, and 3.5 mm is illustrated in Fig. 2(a) and its corresponding value in dB is represented in Fig. 2(b). Best results have been achieved at an optimum length $W_4 = 2.5$ mm. Further increase or decrease in parameter length results in an impedance mismatch.

Theory of characteristics mode (TCM) describes the current patterns and existence of the resonant modes in the B-shaped antenna. TCM can be obtained by solving the eigenvalue equation [36, 37]

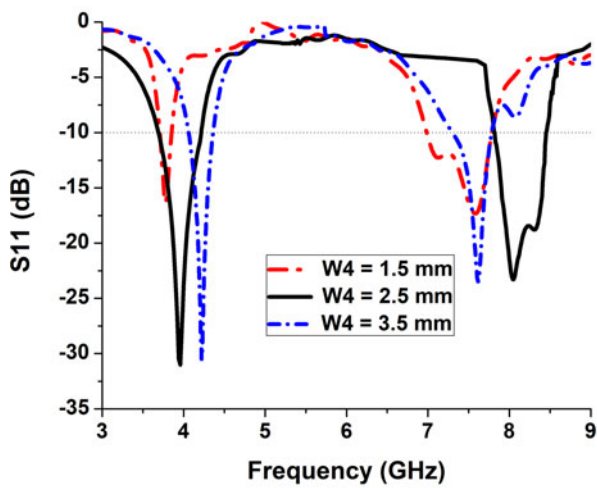
$$XJ_n = \lambda_n R J_n, \quad (1)$$

where J_n represents characteristic currents, λ_n is the eigenvalue, X and R represent the imaginary and real part of the generalized impedance.

A large quantity of modes can be calculated at any operating frequency. However, modes close to the operating frequency represent significant importance and calculated by the n modal



(a)



(b)

Fig. 2. Effect of change in the parameter W_4 on the reflection coefficient (a) plotted on Smith chart (b) plotted in dB.

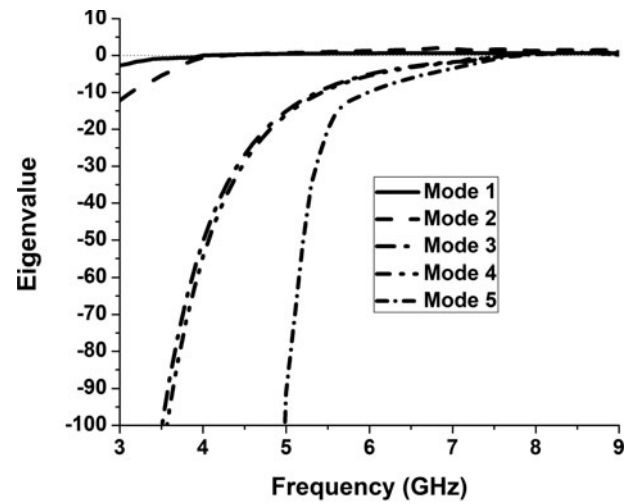


Fig. 4. Eigenvalue of the proposed B-shaped antenna unit cell.

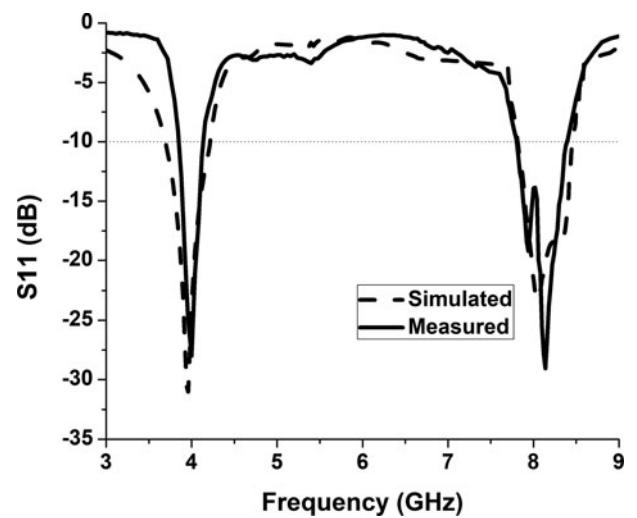


Fig. 5. Reflection coefficient of the proposed B-shaped antenna array.

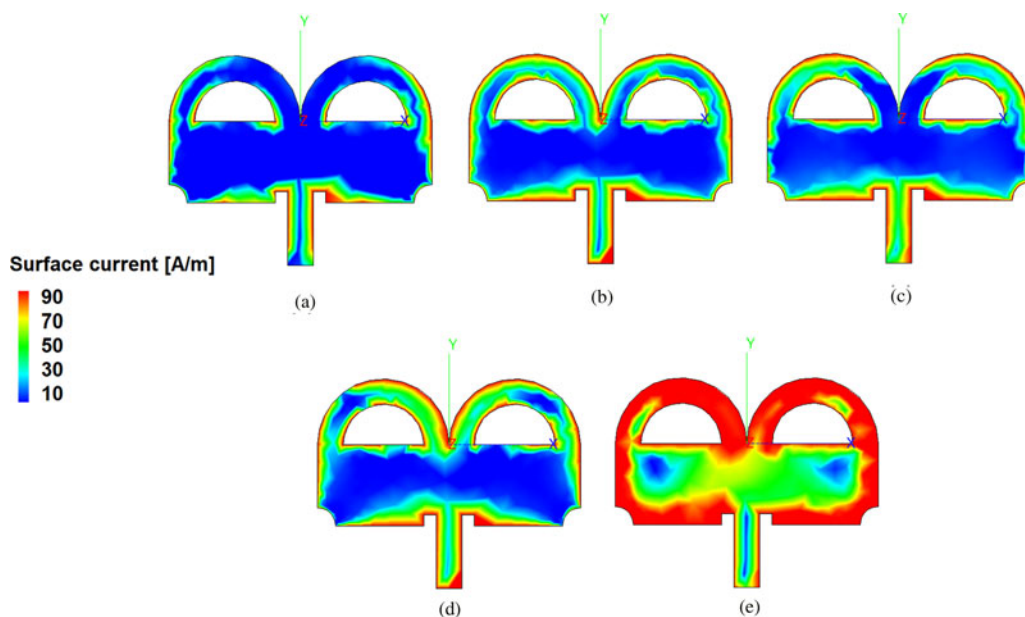


Fig. 3. Surface current density of B-shaped antenna unit-cell resonance at (a) mode 1, (b) mode 2, (c) mode 3, (d) mode 4, and (e) mode 5.

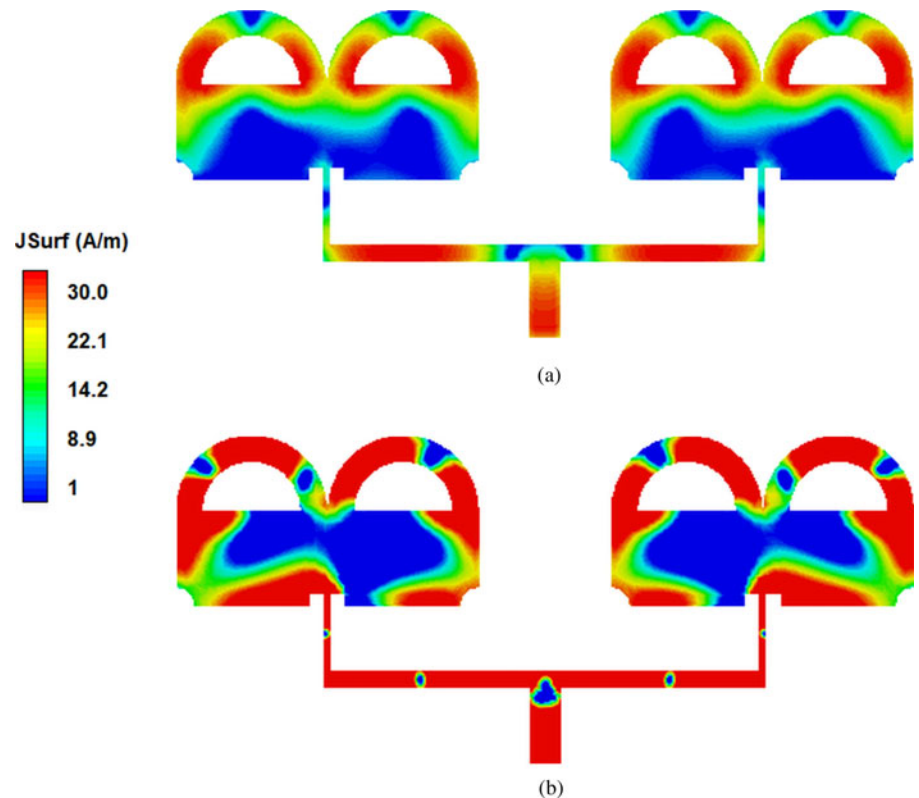


Fig. 6. Surface current distribution at (a) 4 GHz, (b) 8 GHz.

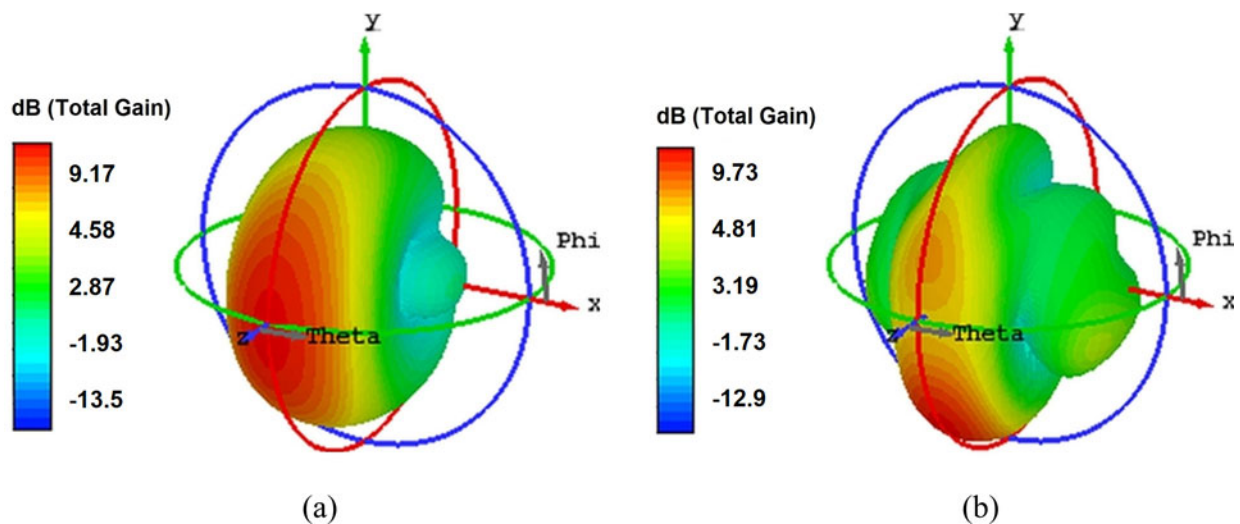


Fig. 7. 3D radiation pattern of the proposed B-shaped antenna array at (a) 4 GHz, (b) 8 GHz.

significance (MS) equation:

$$MS = \frac{1}{|1 + j\lambda_n|}. \quad (2)$$

A mode resonates when its eigenvalue (λ_n) is zero and MS equals to 1. TCM analysis of B-shaped unit cell has been performed in FEKO [38] and illustrated in Fig. 3. Surface current flows along the edges of the B-shaped unit cell in case of mode 1, mode 2, mode 3, and mode 4, respectively, as shown in Figs 3(a)–3(d). However, a strong surface current has been observed along the two annular-strip lines in case of mode 5 as illustrated

in Fig. 3(e). The eigenvalue of the first five resonant modes of the B-shaped antenna unit cell is presented in Fig. 4. A mode resonates when its eigenvalue is zero [39]. For the proposed B-shaped structure, mode 1 and mode 2 resonate at 3.9 and 4.1 GHz, respectively. Mode 3, mode 4, and mode 5 resonate at 7.7, 7.8, and 8 GHz.

The proposed antenna array has been fabricated and the simulated results have been compared with the measured results as shown in Fig. 5. The measured results are in good agreement with the simulated results. The measured impedance bandwidth reference -10 dB is observed at 3.84–4.16 GHz (320 MHz) and 7.78–8.38 GHz (600 MHz), respectively.

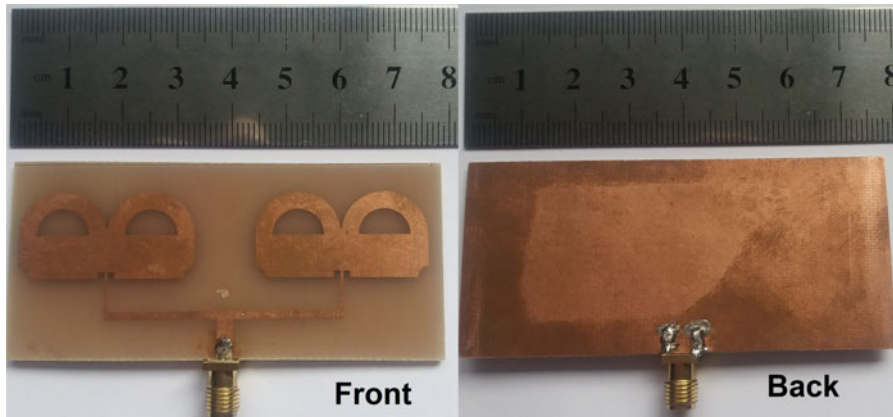


Fig. 8. Prototype of fabricated 1×2 B-shaped antenna array.

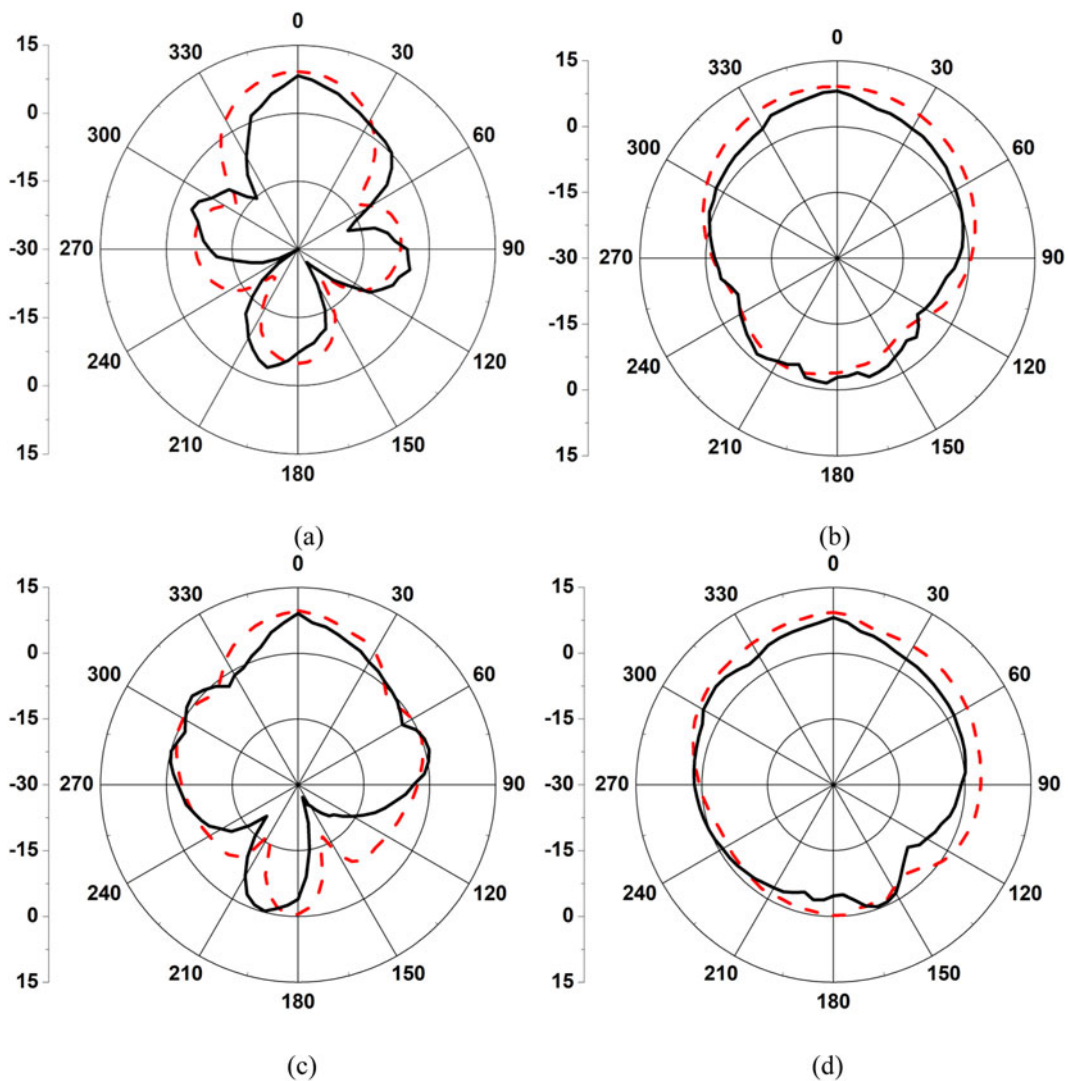


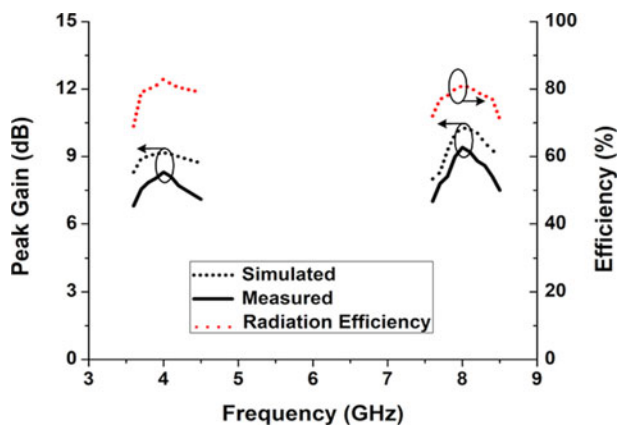
Fig. 9. Radiation pattern of B-shape antenna array: (a) E-plane at 4 GHz, (b) H-plane at 4 GHz, (c) E-plane at 8 GHz, and (d) H-plane at 8 GHz (--- simulated, - - - measured).

Surface current distribution of the B-shaped antenna array has been performed as shown in Fig. 6. At 4 GHz, maximum surface current flows along some portion of annular-shaped strip lines

and T-shaped matching network as shown in Fig. 6(a). Strong surface current flows in the B-shaped antenna array at 8 GHz as depicted in Fig. 6(b).

Table 2. Comparison with recently published dual-band antenna array

Reference number	Antenna size (λ_o)	Operating bands (GHz)	Antenna structure	Peak gain (dB)	Peak efficiency
[24]	$1.12\lambda_o \times 1.12\lambda_o$	1.65–1.67, 1.75–1.76 (Dual-band)	Helical antenna array	8.5	86%
[25]	$2.83\lambda_o \times 1.63\lambda_o$	5.1–5.2, 6.8–6.9, 7.3–7.5 (Tri-band)	Coaxial continuous transverse stub antenna array	7.5	95.9%
[27]	$1.76\lambda_o \times 1.76\lambda_o$	2.6–3.5, 2.5–3.8 (Dual-band)	Tightly coupled dipole array	11.2	80%
[28]	$0.64\lambda_o \times 0.64\lambda_o$	0.69–0.96, 3.5–4.9 (Dual-band)	Shared-aperture antenna array	9.4	Not given
[30]	$1.47\lambda_o \times 1.96\lambda_o$	2.4–2.48, 3.3–3.8 (Dual-band)	Folded dipole antenna array	17.3	Not given
[32]	$0.99\lambda_o \times 0.86\lambda_o$	3.5–3.6, 5.8–6.1 (Dual-band)	Dome-shaped antenna array	7.8	Not given
Proposed work	$1.04\lambda_o \times 0.48\lambda_o$	3.8–4.14, 7.78–8.38 (Dual-band)	B-shaped patch antenna array	9.4	82.5%

**Fig. 10.** Gain and efficiency of the proposed antenna array.

The simulated three-dimensional radiation patterns of the proposed B-shaped antenna array have been displayed in Fig. 7. The peak gain at 4 GHz is 9.17 dB as depicted in Fig. 7(a), whereas the peak gain at 8 GHz is 9.73 dB as shown in Fig. 7(b). The fabricated prototype of 1×2 B-shaped antenna array is shown in Fig. 8.

The radiation pattern of the proposed antenna array has been measured in the anechoic chamber with dimensions $9 \times 4.5 \times 4.9 \text{ m}^3$. The measured radiation patterns and the simulated radiation patterns of B-shaped antenna array have been compared in Fig. 9. E-plane radiation pattern is directional whereas the H-plane radiation pattern is omni-directional. At 4 GHz, peak gain 8.3 dB occurs at 0° , whereas minimum gain -29.5 dB occurs at 240° as shown in Fig. 9(a). At 8 GHz, peak gain 9.4 dB exists at 0° , whereas minimum gain -27.1 dB exists at 160° as depicted in Fig. 9(c).

Peak gain and radiation efficiency of the proposed antenna array are shown in Fig. 10. Measured peak gain ranges 7.5–8.3 and 7.8–9.4 dB at 3.7–4.2 GHz and 7.7–8.4 GHz, respectively. The difference between the measured and simulated results is due to the fabrication tolerance. Measured radiation efficiency ranges 77.3–82.5% in the operating bands.

The comparison of the proposed B-shaped antenna array with the existed literature has been reported in Table 2, where λ_o denotes

free space wavelength at the lowest frequency. The table shows that the proposed antenna array is compact and possesses better gain than [24, 25, 32]. Peak efficiency of the proposed antenna is comparable with [27]. Moreover, the impedance bandwidth (reference -10 dB) is better than [24, 25, 30, 32], respectively.

Conclusion

We hereby proposed a dual-band 1×2 B-shaped patch antenna array. The measured results show impedance bandwidths 320 and 600 MHz at 3.84–4.16 and 7.78–8.38 GHz. Measured peak gain at 4 and 8 GHz is 8.3 and 9.4 dB whereas radiation efficiency is 82.5 and 81.2%, respectively. The dimension of the proposed antenna array is $78 \times 36 \text{ mm}^2$. The results indicate the proposed antenna array is a good candidate for the satellite communication applications.

References

- Maral G and Bousquet M (2009) *Satellite Communications Systems: Systems, Techniques and Technology*. 5th ed., Hoboken, NJ, USA: Wiley.
- Peebles PZ (1998) *Radar Principles*. New York, NY: John Wiley.
- ST TYCZ (1990) Fixed satellite service frequency allocations and orbit assignment procedures for commercial satellite systems. *Proceedings of IEEE* 78, 1283–1288.
- Pozar DM and Targonski SD (2001) A shared-aperture dual-band dual polarized microstrip array. *IEEE Transactions on Antennas Propagation* 49, 150–157.
- Shafai LL, Chamma WA, Barakat M, Strickland PC and Seguin G (2000) Dual-band dual-polarized perforated microstrip antennas for SAR applications. *IEEE Transactions on Antennas Propagation* 48, 58–66.
- Wang BF and Lo YT (1984) Microstrip antennas for dual-frequency operation. *IEEE Transactions on Antennas Propagation* 32, 938–943.
- Singh G, Kanaujia BK, Pandey VK, Gangwar D and Kumar S (2019) Design of compact dual-band patch antenna loaded with D-shaped complementary split ring resonator. *Journal of Electromagnetic Waves Applications* 33, 1–15.
- Mishra B, Patel AK and Singh R (2020) Circularly polarized defected ground stub-matched triple-band microstrip antenna for C- and X-band applications. *Microwave and Optical Technology Letters* 62, 3301–3309.
- Mukherjee B (2015) A novel half hemispherical dielectric resonator antenna with array of slot loaded with a circular metallic patch for wireless applications. *International Journal of Electronics and Communications* 69, 1755–1759.

10. Ojaroudi N, Ghadimi N, Ojaroudi Y and Ojaroudi S (2014) An omnidirectional PIFA for downlink and uplink satellite applications in C-band. *Microwave and Optical Technology Letters* **56**, 2684–2686.
11. Chen Y-Y, Jiao Y-C, Zhao G, Zhang F, Liao Z-L and Tian Y (2011) Dual-band dual-sense circularly polarized slot antenna with a C-shaped grounded strip. *IEEE Antennas and Wireless Propagation Letters* **10**, 915–918.
12. Dai X-W, Zhou T and Cui G-F (2016) Dual-band microstrip circular patch antenna with monopolar radiation pattern. *IEEE Antennas and Wireless Propagation Letters* **15**, 1004–1007.
13. Vallappil AK, Khawaja BA, Khan I and Mustaqim M (2017) Dual-band Minkowski–Sierpinski fractal antenna for next generation satellite communications and wireless body area networks. *Microwave and Optical Technology Letters* **60**, 171–178.
14. Zheng L and Gao S (2011) Compact dual-band printed square quadrifilar helix antenna for global navigation satellite system receivers. *Microwave and Optical Technology Letters* **53**, 993–997.
15. Chiu C-N and Chuang W-H (2009) A novel dual-band spiral antenna for a satellite and terrestrial communication system. *IEEE Antennas and Wireless Propagation Letters* **8**, 624–626.
16. Asif SM, Iftikhar A, Khan SM, Usman M and Braaten BD (2016) An E-shaped microstrip patch antenna for reconfigurable dual-band operation. *Microwave and Optical Technology Letters* **58**, 1485–1490.
17. Zhang T, Hong W, Zhang Y and Wu K (2014) Design and analysis of SIW cavity backed dual-band antennas with a dual-mode triangular-ring slot. *IEEE Transactions on Antennas Propagation* **62**, 5007–5016.
18. Barik RK, Cheng QS, Dash SKK, Pradhan NC and Karthikeyan SS (2020) Compact high-isolation self-diplexing antenna based on SIW for C-band applications. *Journal of Electromagnetic Waves Applications* **34**, 960–974.
19. Tan W and Shen Z (2017) A dual-band dual-sleeve monopole antenna. *IEEE Antennas and Wireless Propagation Letters* **16**, 2951–2954.
20. Wang H, Liu S-F, Zhang L, Li P, Chen L and Shi X-W (2015) Compact wideband and dual-band antenna with directional patterns. *Microwave and Optical Technology Letters*, **57**, 2742–2745.
21. Tiang JJ, Islam MT, Misran N and Mandeep JS (2011) Circular microstrip slot antenna for dual-frequency RFID application. *Progress in Electromagnetics Research* **120**, 499–512.
22. Vijayvergiya PL and Panigrahi RK (2017) Single-layer single-patch dual band antenna for satellite applications. *IET Microwave Antennas and Propagation* **11**, 664–669.
23. Swetha A and Naidu KR (2020) Miniaturized antenna using DGS and meander structure for dual-band application. *Microwave and Optical Technology Letters* **62**, 3556–3563.
24. Yu J and Lim S (2014) Design of a dual-band, electrically small, parasitic array antenna. *IEEE Antennas and Wireless Propagation Letters* **13**, 1453–1456.
25. Prakash PJV and Srinivasan R (2014) Miniaturised multiband two-element coaxial continuous transverse stub antenna for satellite C-band applications. *IET Microwave Antennas and Propagation* **8**, 474–481.
26. Yeung SH, Lamperez GL, Sarkar TK and Palma MS (2014) Thin and compact dual-band four-element broadside patch antenna arrays. *IEEE Antennas and Wireless Propagation Letters* **13**, 567–570.
27. Yang X, Qin P-Y, Liu Y, Yin Y-Z and Guo YJ (2018) Analysis and design of a broadband multifeed tightly coupled patch array antenna. *IEEE Antennas and Wireless Propagation Letters* **17**, 217–220.
28. Chen Y, Zhao J and Yang S (2019) A novel stacked antenna configuration and its applications in dual-band shared-aperture base station antenna array designs. *IEEE Transactions on Antennas Propagation* **67**, 7234–7241.
29. Mao C-X, Gao S, Wang Y, Chu Q-X and Yang X-X (2017) Dual-band circularly polarized shared-aperture array for C-/X-band satellite communications. *IEEE Transactions on Antennas Propagation* **65**, 5171–5178.
30. Wang Z, Zhang G-X, Yin Y and Wu J (2014) Design of a dual-band high-gain antenna array for WLAN and WiMAX base station. *IEEE Antennas and Wireless Propagation Letters* **13**, 1721–1724.
31. Sah S, Mittal A and Tripathy MR (2019) High gain dual band slot antenna loaded with frequency selective surface for WLAN/ fixed wireless communication. *Microwave and Optical Technology Letters* **61**, 519–525.
32. Dewan R, Rahim SKA, Malek F, Ausordin SF, Yusuf AA and Azemi SN (2013) A dual-band array antenna using dome-shaped radiating patches. *Microwave and Optical Technology Letters* **55**, 2680–2686.
33. Wu J, Wang C and Guo YX (2019) Dual-band co-aperture planar array antenna constituted of segmented patches. *IEEE Antennas and Wireless Propagation Letters* **19**, 257–261.
34. Pozar DM (1998) *Microwave engineering*. New York: Wiley.
35. **Computer Simulation Technology (CST)** (2016) Microwave Studio Suite. Accessed 15 April 2020. Available at <http://www.cst.com>.
36. Bouezzedine M and Schroeder WL (2016) Design of a wideband, tunable four-port MIMO antenna system with high isolation based on the theory of characteristic modes. *IEEE Transactions on Antennas and Propagation* **64**, 2679–2688.
37. Chen Y and Wang C-F (2015) *Characteristic Modes: Theory and Applications in Antenna Engineering*. Hoboken, NJ: John Wiley and Sons, Inc.
38. **Altair Engineering FEKO** (2017) Accessed 15 April 2020. [Online] Available at <http://www.altairhyperworks.com/product/FEKO>.
39. Hassan MM, Zahid Z, Khan AA and Maqsood M (2019) A wideband loop-type ground radiation antenna using ground mode tuning and optimum impedance level. *Microwave and Optical Technology Letters* **61**, 2056–2061.



Muhammad Mateen Hassan received his Electronics Engineering degree from the Wah Engineering College, University of Wah, Pakistan, in 2009 and the M.S. degree in Electrical Engineering from the Technische Universität Chemnitz, Germany, in 2013. Currently, he is pursuing his Ph.D. degree from the National University of Sciences and Technology, Islamabad, Pakistan. His research interests are in the field of MIMO antennas, reconfigurable antennas, micro-electro-mechanical systems (MEMS) for RF applications, and nanotechnology.



Muzhair Hussain did his M.S. degree from the National University of Sciences and Technology (NUST), Islamabad, Pakistan, in 2019. He is currently working as a Lab Engineer in NUML, Islamabad.



with UET Taxila, Pakistan.

Dr. Adnan Ahmed Khan did his B.E. degree in Electrical (Telecomm) Engineering from the National University of Sciences and Technology, Pakistan. He received his Master's degree in Computer Engineering from the University of Engineering and Technology, Taxila. He received his Ph.D. degree in Computer Engineering from the Center of Advanced Studies in Engineering, affiliated



Dr. Imran Rashid did his B.E. degree in Electrical (Telecomm) Engineering from the National University of Sciences and Technology, Pakistan, in 1999. He received his M.Sc. degree in Telecomm Engineering (Optical Communication) from D.T.U, Denmark in 2004 and his Ph.D. degree in Mobile Communication from the University of Manchester, UK in 2011.



Dr. Farooq Ahmed Bhatti has got his Master degree in Solid State Physics from Punjab University Lahore, Pakistan in 1979. He did his Ph.D. degree in Radio Physics (RF Electronics) specializing in Microwave and Millimeter-wave Sources from the Department of Communication Engineering Shanghai University PR, China in 1992. He did his Post Doc in Millimeter-wave Devices from the

Centre for Microwave and Millimeter-wave Circuit Design and Applications,

University of Manchester, UK. He joined the National University of Sciences and Technology, Islamabad, Pakistan in 1995. Presently he is an Associate Professor at the National University of Sciences and Technology, Islamabad, Pakistan.